ACS OMEGA

Open Access

http://pubs.acs.org/journal/acsodf

Article

Highly Accurate and Robust Early Stage Detection of Cholangiocarcinoma Using Near-Lossless SERS Signal Processing with Machine Learning and 2D CNN for Point-of-care Mobile Application

Pobporn Danvirutai, Thatsanapong Pongking, Suppakrit Kongsintaweesuk, Somchai Pinlaor, Sartra Wongthanavasu, and Chavis Srichan*

Cite This: *ACS Omega* 2025, 10, 11296−11311

Read Online

ACCESS | Metrics & More | Article Recommendations | Supporting Information

ABSTRACT: Introduction: Cholangiocarcinoma (CCA), a malignancy of the bile ducts, presents a significant health burden with a notably high prevalence in Northeast Thailand, where its incidence ratio is 85 per 100,000 population per year. The prognosis for CCA patients remains poor, particularly for proximal tumors, with a dismal 5-year survival rate of just 10%. The challenge in managing CCA is exacerbated by its typically late detection, contributing to a high mortality rate. Current screening methods, such as ultrasound, are insufficient, as many CCA patients do not exhibit prior symptoms or detectable liver fluke (*Opisthorchis viverrini:* OV) infections, underscoring the urgent need for alternative early detection methods. Methods: In this study, we introduce a novel approach utilizing surface-enhanced Raman spectroscopy (SERS) combined with near-lossless signal compression via discrete wavelet transform (DWT) together with 2D CNN for the first time. Hamster serums of different stages were collected as the data set. DWT was employed for feature extraction, enabling the capture of the entire SERS spectrum, unlike traditional methods like PCA and LDA, which focus only on specific peaks. These features were used to train a 2D convolutional neural network (2D CNN), which is particularly robust against translation, rotation, and scaling, thus effectively addressing the SERS peak shifting issues. We validated our approach using gold-standard histology, and notably, our method could detect CCA at an early stage. The ability to identify CCA at the early stage significantly improves the chances of successful intervention and patient outcomes. Results and conclusion: Our results demonstrate that our method, combining SERS with extremely compact wavelet feature extraction and 2D CNN, outperformed other approaches (PCA + SVM, PCA + 1D CNN, PCA + 2D CNN, LDA + SVM, and DWT + 1D CNN), achieving performance of 95.1% accuracy, 95.08% sensitivity, 98.4% specificity, and an area under the curve (AUC) of 95%. The trained model was further deployed on a server and mobile application interface, paving the way for future field experiments in rural areas and home-use potential point-of-care services.

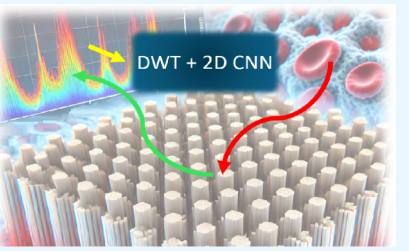

1. INTRODUCTION

Cholangiocarcinoma (CCA) is a high-mortality rate cancer with 5-year survival rate at only 10% in proximal tumors[1] and typically less than 20% in recent years.[2] It represents a significant public health challenge, particularly in Northeast Thailand, where it has a high prevalence, with an incidence ratio of 85 per 100,000 population per year.[3] CCA, a highly malignant tumor of the bile ducts, often diagnosed at an advanced stage due to its insidious onset and nonspecific symptoms. This late detection leads to high mortality rates as many patients miss the opportunity for early intervention. Early detection of CCA, pre-CA, and inflammation or cholangitis is therefore crucial for improving patient outcomes. Current diagnostic methods for CCA face several limitations, normally late stage were detectable. In addition, ultrasound screening for liver fluke (OV) is insufficient since, there are more portion of patients that could develop CCA without OV infection. CCA was mentioned as a "silent killer", hard to detect, in the report.[4]

Current detection methods primarily rely on imaging techniques such as ultrasonography, computed tomography (CT), and magnetic resonance imaging (MRI). While these methods can effectively visualize tumors, their ability to detect CCA at an early stage is limited, particularly for small or infiltrative tumors, resulting in delayed diagnosis and treatment.[5,6] Endoscopic procedures like endoscopic retrograde cholangiopancreatography[7] and percutaneous transhepatic cholangiography (PTC) offer more direct visualization and

Received: December 7, 2024
Revised: February 28, 2025
Accepted: March 5, 2025
Published: March 12, 2025

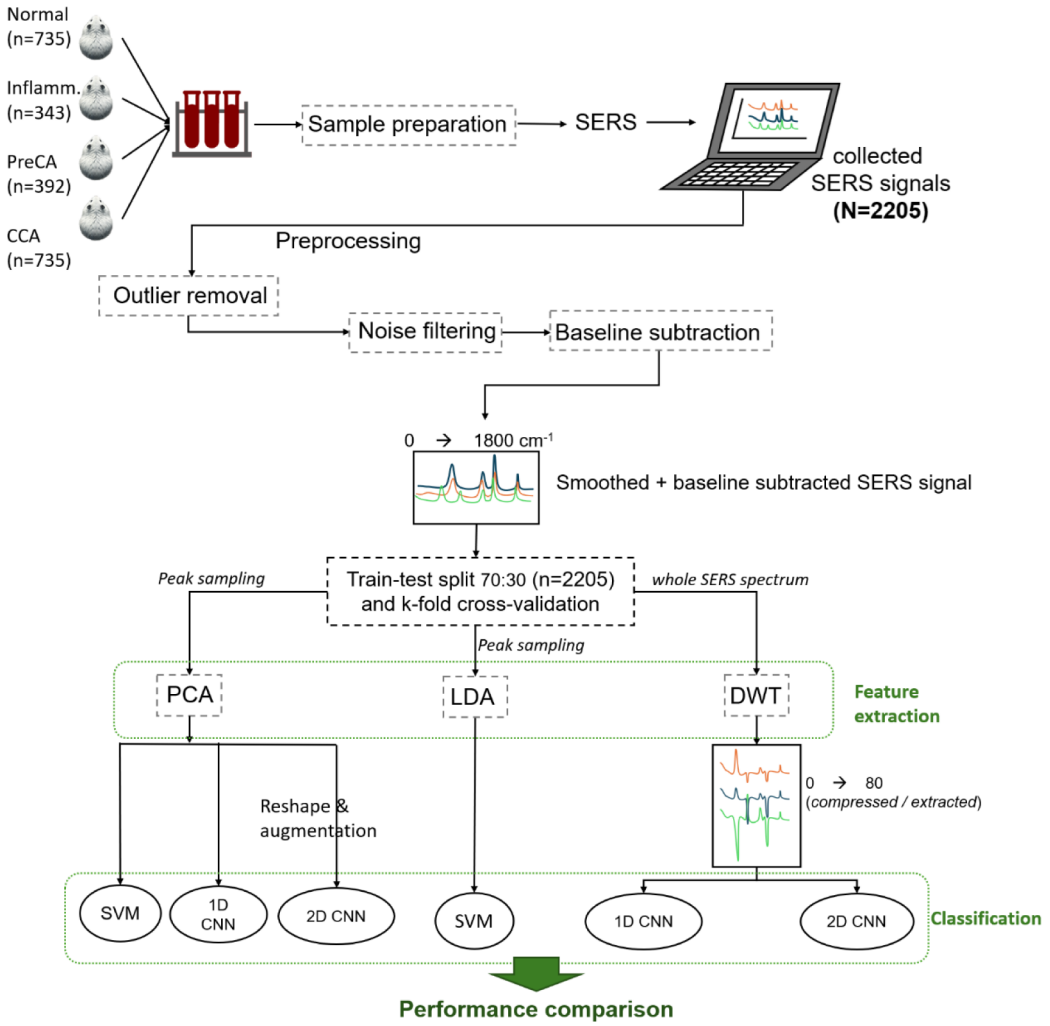

Figure 1. Workflow and study design. Blood serum was collected from hamsters at four stages. A total of 2,205 SERS signals were collected from hamster serum distributed among four stages, each of which were measure 49 times over different spatial conditions. The SERS signals underwent preprocessing, including outlier removal, noise filtering, and Raman baseline subtraction. The preprocessed SERS signals (n = 2205) were then used for train-test splitting and 10-fold cross-validation. Three feature extraction methods were employed in this study: PCA, LDA, and the proposed DWT. PCA and LDA, as conventional methods, rely on significant peak sampling from the SERS signals, ignoring most of the Raman/SERS information. In contrast, DWT utilizes multiresolution eigenfunctions to compress the signal from its original 1 × 18,000 size (10 floating digits, 1,800 numbers) down to a 1 × 80 size feature. The performance of each feature extraction and classification method was studied and compared.

the possibility of obtaining biopsy samples.[8] However, these methods are invasive, carry risks such as infection and pancreatitis, and may still miss early stage disease.[9,10]

Serum biomarkers, including carbohydrate antigen 19-9 (CA 19-9) has been used as noninvasive tools for CCA detection.[11] Despite their widespread use, these biomarkers suffer from low specificity and sensitivity, often leading to false positives and negatives, particularly in early stage CCA. Therefore, biomarker detection approaches require employment of multiple-biomarker which will suffers from high cost and time building antibody-based sensing materials.[12] Recent advances in molecular diagnostics, such as the analysis of circulating tumor DNA (ctDNA) and microRNAs, have shown potential as more sensitive and specific noninvasive biomarkers for early CCA detection. Using ctDNA and microRNAs as the CCA indicators face limitations like low ctDNA or microRNA levels compared to other biomarkers and thus need for further validation.[13,14] The clinical implementation of these approaches face challenges such as high cost, technical complexity, and the need for further validation in large patient cohorts.[15]

Surface-enhanced Raman spectroscopy (SERS) has emerged as a powerful analytical technique in cancer diagnostics,[16] demonstrating its potential for detecting various types of cancer through the analysis of serum samples and specific biomarkers. The enhanced sensitivity and specificity of SERS, compared to conventional Raman spectroscopy, have made it an attractive tool for early cancer detection and staging. Numerous studies have reported successful applications of SERS in identification of cancers including breast,[17−19] lung,[20,21] prostate,[22,23] hepatocellular carcinoma,[24,25] and colorectal cancer,[26,27] showing its versatility and effectiveness in oncological research. Despite the widespread use of SERS in cancer diagnostics, its application in the detection and classification of cholangiocarcinoma (CCA) remains unexplored. This gap in the literature presents an opportunity for our work to address the challenges associated with CCA diagnosis and stage classification. While conventional Raman

https://doi.org/10.1021/acsomega.4c11078
ACS Omega 2025, 10, 11296−11311

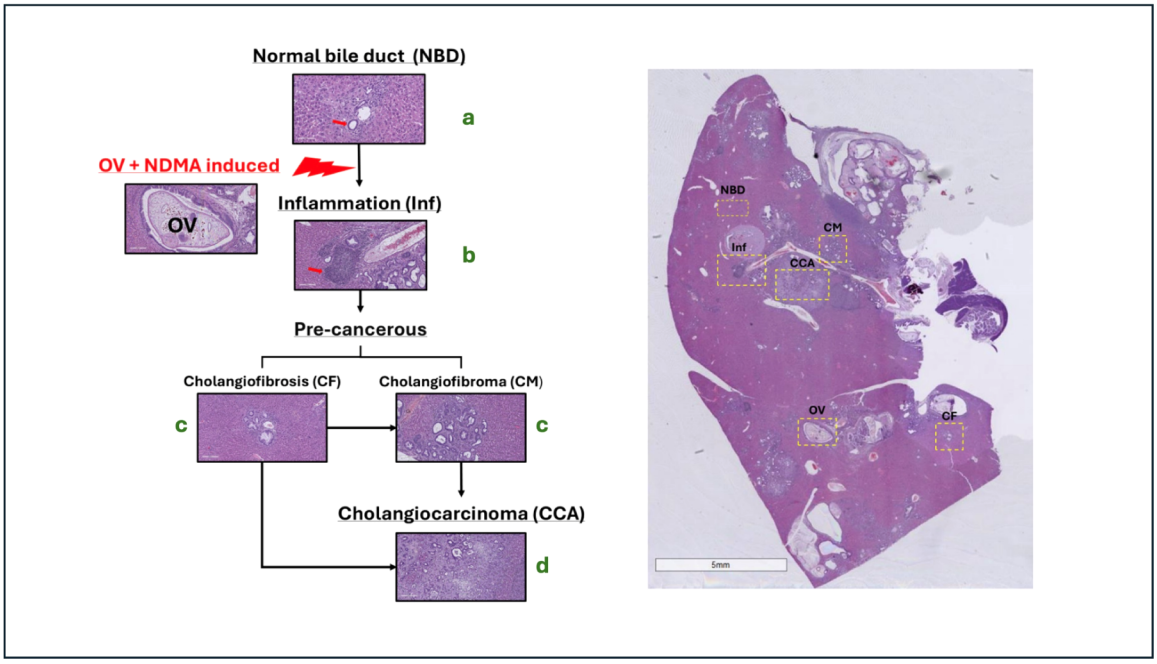

Figure 2. Left figure: H&E staining of tissue samples reveals the progression of cholangiocarcinoma (CCA) in hamster liver which were divided into four main stages (a–d): normal, inflammation, precancerous and CCA. Right figure: Location of normal and abnormal bile duct in hamster liver.

spectroscopy has been employed for CCA detection,[28−30] the results have been limited by the similarity between CCA and normal serum spectra which are hardly distinguishable by human. This similarity poses a significant challenge in development of signal processing, feature extraction and machine learning methods to optimize the CCA classification performance which will be reported in this work.

The limitations of conventional Raman spectroscopy in CCA detection underscore the need for more advanced techniques, such as SERS, coupled with sophisticated signal processing and classification methods. The enhanced sensitivity of SERS could potentially overcome the spectral similarities observed in conventional Raman analysis, providing more distinct and informative spectral features. However, to fully harness the capabilities of SERS for CCA classification, particularly in serum samples, it is crucial to develop and implement high-efficiency signal processing algorithms and accurate classification techniques.

This study is the first to report the use of surface-enhanced Raman Spectroscopy (SERS) for CCA classification using DWT + 2D CNN on serum data set. While SERS significantly enhances Raman signals, it struggles with peak shifting, which compromises its robustness. To address this issue, we propose a novel approach combining SERS with wavelet transform for feature extraction and a 2D convolutional neural network (CNN) for classification.[31,32] The 2D CNN is invariant to translation (SERS shifting), as well as scaling and noise, enhancing the reliability of the analysis. Additionally, the wavelet transform allows for near-lossless feature extraction from the SERS spectrum, overcoming limitations of traditional peak sampling methods used in PCA and LDA postprocessing for Raman signals.

Other methods for CCA detection, such as direct Raman spectroscopy and electrochemical sensing, have been explored in recent literature. While these studies have made significant contributions to CCA detection and classification, each approach has its limitations. Our proposed method aims to address these challenges and potentially improve diagnostic accuracy by leveraging the strengths of SERS, wavelet transform, and 2D CNN.

The proposed method integrates the high sensitivity of SERS, the whole-spectrum coverage feature extraction capabilities of wavelet transforms, and the strengths of two-dimensional CNNs which is invariant to scaling and translation (SERS peak shifting) and finally implemented them into a mobile application. The result is a portable, accessible, and accurate tool for early CCA detection, which achieved the greatest performance in comparison with other SERS + signal processing and machine learning approaches such as PCA or LDA with support vector machine (SVM).

2. MATERIALS AND METHODS

In this study, we employed surface-enhanced Raman spectroscopy (SERS) combined with advance feature extraction techniques and neural networks for the classification of cholangiocarcinoma (CCA). SERS was chosen for its ability to significantly enhance Raman signals, though it presents challenges such as peak shifting, which can compromise the robustness of the analysis. To overcome these challenges, we implemented a 2D convolutional neural network (CNN), selected for its translation invariance and robustness to scaling and noise, making it particularly effective in handling the variability inherent in SERS data. Additionally, we applied wavelet transform for near-lossless feature extraction from the SERS spectra, addressing the limitations of traditional peak sampling methods used in Principal Component Analysis (PCA) and Linear Discriminant Analysis (LDA), which may miss significant spectral information. Following the preparation of hamster serum samples, SERS measurements were conducted, and the signal processing and feature extraction steps were meticulously carried out. We then compared the performance of discrete wavelet transform combined with 2D

https://doi.org/10.1021/acsomega.4c11078
ACS Omega 2025, 10, 11296−11311

CNN against other methods, including LDA or PCA combined with support vector machines (SVM), PCA combined with 1D CNN, and PCA combined with 2D CNN, to ensure the most accurate classification of CCA. Overall picture of methodology of this study can be summarized in Figure 1.

2.1. Sample Preparation. *2.1.1. Histopathological Manifestation.* A total of 45 H&E-stained hamster liver tissue samples were analyzed, including 15 samples from the control group and 30 samples from the OV+NDMA-induced groups (1, 3, 4, and 5 months). All samples from the induced groups exhibited inflammatory lesions in the tissue. However, precancerous such as cholangiofibrosis and cholangioblastoma and CCA lesions, were observed only after three months of induction. Pathological stages' images were placed in Figure 2.

2.1.2. Animal and Ethical Statement. The study involved a total of 45 male Syrian golden hamsters (*Mesocricetus auratus*), aged 4−6 weeks and weighing between 80 and 100 g, selected at random. These were raised at the Faculty of Medicine's Animal Unit of Khon Kaen University in Thailand. Before conducting the experiment, they were acclimatized for at least 5 days. Each hamster was kept in a hygienic controlled environment maintained at 23 °C (±2 °C), relative humidity range of 30% to 60%, and light-dark cycle of 12 h each. They were fed with commercial pellet meal (CP-SWT, Thailand) and had ad libitum access to water.

The stainless-steel cages were cleaned weekly with detergent and disinfected using Dettol (Dettol, Thailand) to prevent bacterial infection. The sawdust bedding was changed two times a week. The study protocol (IACUC-KKU-56/66) underwent scrutiny by Khon Kaen University's Animal Ethics Committee in accordance with the ethical guidelines for the use of animals in experiments described by National Research Council, Thailand.

2.1.3. Pathological Experimental Design. Forty-five hamsters were randomly divided into two groups: (1) a normal control group (n = 15) and (2) an experimental group infected with *Opisthorchis viverrini* (OV) and exposed to N-nitrosodimethylamine (NDMA) (n = 30). The experimental group (OV+NDMA) was monitored and maintained for one to five months to study the time-course development of cholangiocarcinoma (CCA). The normal control group was maintained in parallel to serve as the cancer-free control.

OV were extracted from naturally infected cyprinid fish using a pepsin digestion process. The metacercariae were isolated and counted after digesting the fish in a solution containing 0.25% pepsin and 1.5% hydrochloric acid (Wako Pure Chemical Industries, Osaka, Japan) in 0.85% sodium chloride. Each hamster received 50 live O. viverrini metacercariae via intragastric gavage. The drinking water for the OV+NDMA group contained NDMA at a concentration of 12.5 ppm (ppm).

At the end of the study, all hamsters were fasted for 1 day before euthanasia. The hamsters were anesthetized and euthanized by isoflurane inhalation. Blood was collected via cardiac puncture and allowed to coagulate. The blood was then centrifuged for 10 min at 4 °C and 3500 rpm. The serum was separated, aliquoted, and stored at −20 °C for subsequent Raman spectroscopy analysis.

2.2. Hematoxylin and Eosin (H&E) Staining. H&E staining enhances the visibility of tissue sections, allowing for detailed examination and analysis of their structural and pathological features. For this process, paraffin-embedded tissues from each group of hamsters were treated with xylene to dissolve the paraffin, typically for two intervals of 5 min each. The tissue slices were then rehydrated through a series of decreasing ethanol concentrations (100%, 95%, and 70%), followed by rinsing in distilled water to remove any remaining ethanol.

Next, the rehydrated tissue sections were stained with hematoxylin for 10 min. After staining, the sections were washed under running water for about 5 min and then treated with an ammonia−water substitute to intensify the blue color of the nuclei. The sections were rinsed again with tap water. Following the hematoxylin staining, the sections were stained with eosin for one to 2 min, which stained the cytoplasmic and extracellular components pink. The sections were then quickly rinsed in distilled water.

After staining, the sections were dehydrated and cleared. They were passed through a series of increasing ethanol concentrations (70%, 95%, and 100%) for 1 min each and then cleared in xylene for two intervals of 1 min each. The stained tissue sections were mounted with a mounting medium and coverslip, preserving the stained tissue for long-term storage and examination under a microscope, enhancing the clarity and contrast of the stained components.

2.3. Preprocessing and Feature Extraction. *2.3.1. Preprocessing.* The raw SERS spectra underwent several preprocessing steps to remove noise and baseline variations, ensuring accurate feature extraction. First, baseline subtraction was performed using the asymmetric least-squares (ALS) method to adjust for any baseline drifts. Next, the spectra were normalized to the total area under the curve to account for intensity variations between samples. Finally, a Savitzky-Golay filter was applied to smooth the spectra, reducing high-frequency noise and enhancing signal clarity. These preprocessing steps were crucial for preparing the data for subsequent wavelet transform and machine learning analysis.

To address the difficulty in distinguishing between the Raman signals of normal and abnormal serum, the raw signals were subjected to discrete wavelet transform (DWT). The wavelet transform, with its multiresolution basis, enhanced the differences in the signals. After wavelet trasform applied to the Raman signal, the signal which appear to be indistinguishable at the first place become discriminable by human eyes. In principle, if human eyes can discriminate then AI model can be construct as a classifier.

We imposed quality control standards employed to maintain signal integrity during preprocessing. Outlier identification is based on two principal criteria: first, signals displaying a signal-to-noise ratio (SNR) below 4 dB are discarded to avoid unreliable measurements; and second, spectra presenting anomalous baseline shifts or artifacts (e.g., spikes or dips) are flagged as outliers and removed from subsequent analyses. By adhering to these predefined benchmarks, the data set preserves a consistent level of reliability, ultimately enhancing the robustness and reproducibility of the study's findings.

To handle potential imbalances among the four classes, a dual strategy involving both oversampling and weighted loss functions was implemented during model training. Specifically, oversampling was applied to the minority classes—namely, the precancerous and inflammation groups—to ensure a balanced representation across all categories. In parallel, a weighted cross-entropy loss function was employed to impose a more severe penalty on misclassifications pertaining to these underrepresented classes. This integrated approach was

https://doi.org/10.1021/acsomega.4c11078
ACS Omega 2025, 10, 11296−11311

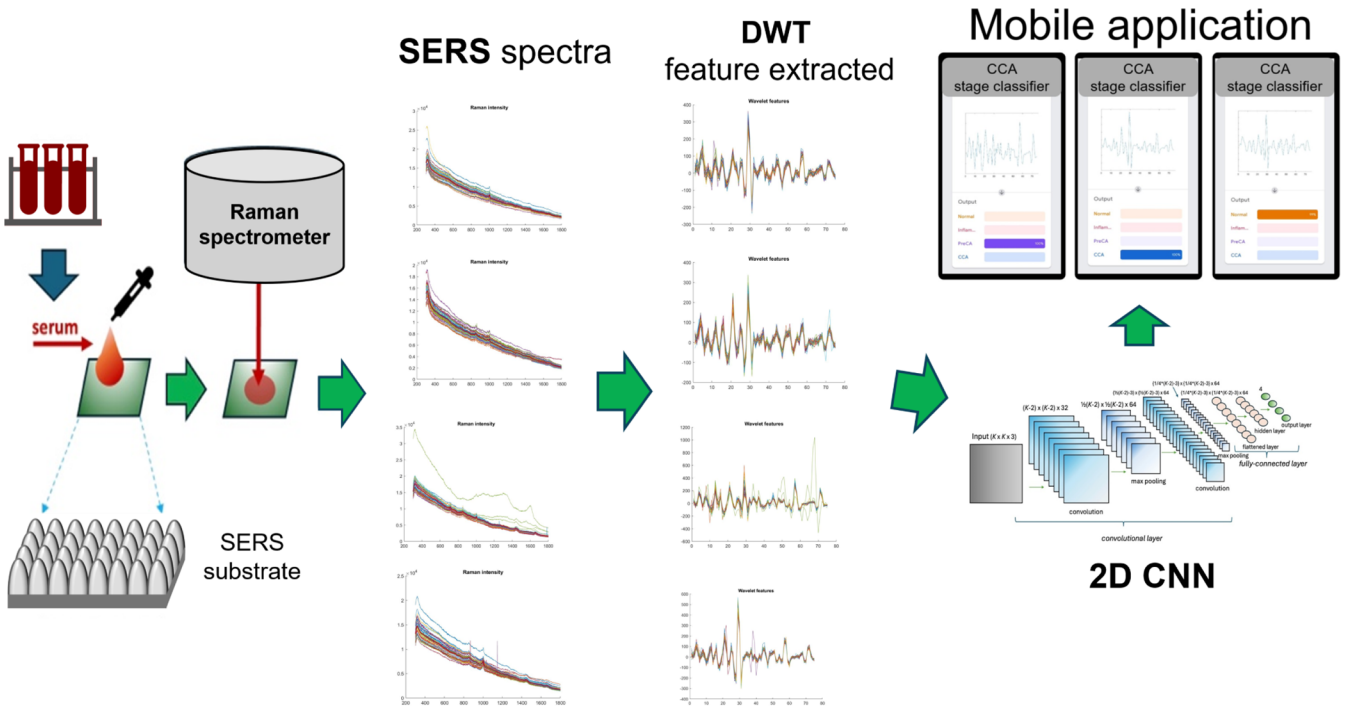

Figure 3. Illustration of the complete process of the CCA classification system. The sequence begins with the application of serum onto a SERS substrate, followed by the collection of SERS signals using a Raman spectrometer. These signals undergo wavelet transform and are processed through convolutional neural networks (CNNs). Finally, a mobile application classifies the Raman signals into four stages: normal, inflammation, precancerous, and cholangiocarcinoma.

essential for reducing bias toward the majority classes and enhancing the overall model sensitivity and performance.

2.3.2. Feature Extraction Using Wavelet Transform. The wavelet transform was integrated into the SERS signal processing pipeline to enhance the discrimination of CCA-related features. Wavelets are mathematical functions that decompose a signal into different scale components, making them effective in analyzing transient, nonstationary, or time-varying phenomena. The core of wavelet theory is multi-resolution analysis (MRA), which allows signals to be decomposed into components at various resolution levels, enabling the simultaneous analysis of coarse and fine signal features.

Given that the signals were in digital format, the discrete wavelet transform (DWT) was utilized for feature extraction from the preprocessed SERS spectra. The choice of the wavelet function and decomposition level is crucial; in this study, the Daubechies (db4) wavelet was selected, and the spectra were decomposed into 80 levels.

A signal $x[n]$ can be decomposed into approximation and detail coefficients through DWT. The approximation coefficients $c_A[k]$ and detail coefficients $c_D[k]$ at level j are computed as follows

$$C_A[k] = \sum_n x[n]\cdot\phi(2^j n - k) \tag{1}$$

$$C_D[k] = \sum_n x[n]\,\psi(2^j n - k) \tag{2}$$

where ϕ and ψ are the scaling and wavelet functions, respectively. In this process, the signal is passed through low-pass and high-pass filters, followed by downsampling by a factor of 2. Lowpass filter, $h[n]$, can be expressed as

$$C_A[k] = \sum_n x[n]\cdot h(2k - n) \tag{3}$$

While the highpass filter, $g[n]$, are expressed by

$$C_D[k] = \sum_n x[n]\cdot g(2k - n) \tag{4}$$

The DWT efficiently compresses the signal while preserving critical information, making it useful for various applications, such as signal compression, noise reduction, and feature extraction. For multilevel decomposition, the coefficient at step j, $C_{A,j}[k]$, can be decomposed further as

$$C_{A,j+1}[k] = \sum_n C_{A,j}[n]\cdot h(2k - n) \tag{5}$$

$$C_{D,j+1}[k] = \sum_n C_{A,j}[n]\cdot g(2k - n) \tag{6}$$

To reconstruct the original Raman or SERS signal, we use inverse discrete wavelet transform

$$x[k] = \sum_n (C_{A,j}[n]\cdot h[2n - k] + C_{D,j}[n]\cdot g[2n - k]) \tag{7}$$

and

$$C_{A,j}[k] = \sum_n C_{A,j+1}[n]\cdot h[n - 2k] + C_{D,j+1}[n]\cdot g[n - 2k] \tag{8}$$

When applied to surface-enhanced raman scattering (SERS) signals, the DWT reduces the size of feature data (from 1800*(10 floating point digits) down to merely 80 in this work) while maintaining essential spectral characteristics. This allows for efficient feature extraction and dimensionality reduction. The DWT-transformed signals were converted to

https://doi.org/10.1021/acsomega.4c11078
ACS Omega 2025, 10, 11296−11311

1D vectors for 1D CNN classification training and 2D images for 2D CNN.

The CCA classification system, illustrated in Figures 1 and 3, begins with the application of serum onto a Surface-Enhanced Raman Scattering (SERS) substrate, followed by the collection of Raman signals using a spectrometer. These signals undergo wavelet transform for feature extraction and are then processed by either support vector machine (SVM), 1D convolutional neural networks (1D CNN), or 2D convolutional neural networks (2D CNN) to distinguish between four stages: normal, inflammation, precancerous (pre-CA), and cholangiocarcinoma. Classification results is output directly from the neural network model used and only DWT + 2D CNN were deployed into mobile application since this proposed method outperform others.

2.3.3. Feature Extraction Using PCA and LDA. Principal component analysis (PCA) and linear discriminant analysis (LDA) are fundamental techniques for feature extraction, particularly in simplifying and enhancing complex data sets for more effective analysis. PCA transforms the original data into a new coordinate system, focusing on capturing the greatest variance along the principal components, which reduces dimensionality by eliminating noise and redundancy. LDA, a supervised method, seeks to maximize the separation between multiple classes by finding linear combinations of features that optimize the ratio of between-class variance to within-class variance. These techniques are especially useful in applications like SERS signal analysis, where the focus traditionally has been on sampling high-intensity peaks, represented as an array of tuples {wavenumber, intensity}. This data set, compiled from these tuples, often neglects the rest of SERS wavenumbers and intensities, which can lead to the loss of potentially valuable information. By applying PCA and LDA, the discriminative power of the extracted features is enhanced, facilitating improved performance in subsequent machine learning models. In this work, we will compare the performance of using PCA, LDA and DWT as feature extractor techniques.

2.4. SERS Preparation and Measurement. *2.4.1. SERS Measurement.* Blood was drawn from each hamster, and serum was separated through centrifugation. The serum samples were then diluted with deionized (DI) water at a 1:10 ratio and dropped onto a silver-nanorod SERS substrate (details in the next section). A 10 μL diluted serum sample was placed onto a glancing-angle deposition (GLAD) silver nanorod SERS substrate (0.25 mm thickness, 2 mm diameter) over a polystyrene glass. To prevent serum evaporation, a quartz coverslip (RS2500, Esco Optics, Oak Ridge, NJ) was placed over the sample well. The diluted serum samples were collected for their Raman or SERS signals using a Horiba XploRA PLUS confocal Raman microscope (Horiba Jobin Yvon, Northampton, UK) equipped with a 50x objective lens (LMPLFL50X, Olympus, St. Joseph, MI) and a 785 nm laser source, ensuring a stable signal through an integrated high-performance system.

Five minutes after each drop, Raman signals were collected over 49 nearby grids, generating Raman intensity data for each serum sample. Each spectrum was recorded in the range of 200−2000 cm^{-1} with an integration time of 1 s and a spectral resolution of 0.1 cm^{-1}, ensuring reproducibility and allowing for outlier rejection. This measurement provided the raw Raman signals necessary for further analysis. However, the pure Raman or SERS signals from normal and abnormal serum samples were mostly indistinguishable by visual inspection, as noted by Suksuratin et al. (2022),[28] posing a challenge for direct interpretation (Figure 4a). To address this, wavelet transform was applied for feature extraction, which allowed for clear discrimination between cholangiocarcinoma (CCA) signals and those from normal and intermediate states, as shown in Figure 4b. SERS spectra samples of the four CCA stages were placed in Figure 4c,e,g, and i. Where the feature extracted signals using discrete wavelet transform were placed in Figure 4d,f,h, and j. This signal processing step was crucial before applying machine learning and classification techniques to the data.

2.4.2. SERS Substrate. The silver nanorod SERS substrate used in this study was purchased from NECTEC under the brand "ONSPEC".[33] The choice of the silver nanorod as the SERS substrate was due to its established reproducibility in SERS applications.[29,30,34−36] These silver nanorods were fabricated using the glancing angle deposition (GLAD) technique, which allows for precise control over nanorod dimensions and spacing, resulting in highly uniform and reproducible SERS substrates.[33] The GLAD method ensures that these nanostructured surfaces exhibit significant enhancement of Raman signals due to their plasmonic properties, enabling sensitive detection of various analytes at low concentrations.[30]

The high tunability of silver nanorod arrays makes them particularly versatile for a wide range of SERS-based sensing and analytical applications.[36] This SERS substrate has demonstrated the ability to detect biomarkers and chemicals without the need for antibody addition. The high sensitivity of SERS allows for the detection of minute biochemical changes associated with CCA, pre-CCA, and cholangitis, making it a powerful tool in the analysis of serum samples.

2.5. Convolutional Neural Network (CNN) for Classification of CCA Stages. Convolutional Neural Networks (CNNs) have revolutionized the field of artificial intelligence, particularly in tasks involving image and pattern recognition. By mimicking the way human vision processes visual information, CNNs can automatically and adaptively learn hierarchical patterns and features from raw data. This ability has enabled CNNs to surpass human expert performance in certain tasks, especially in image classification, where they have demonstrated remarkable accuracy and efficiency. A historical example of this is the 2015 ImageNet Large Scale Visual Recognition Challenge, where a CNN-based system called ResNet achieved an error rate lower than that of human experts for the first time.[31] With their capacity to handle large volumes of data and uncover hidden patterns beyond human perception, CNNs are transforming medical technologies which we will explore one specific task in this work.

2.5.1. One-Dimensional Convolutional Neural Network (1D CNN). One-dimensional CNN was employed to process one-dimensional data, such as discrete wavelet transformed (1D) vectors or PCA vectors, depending on the feature extraction method used. The input to the 1D CNN had a shape consisting of the number of samples, sequence length, and the number of channels. As depicted in Figure 5a, the architecture of the 1D CNN included 8 convolutional layers with 1D kernels that slide along the sequence dimension, applying filters to local patches to capture temporal patterns and dependencies. This method is particularly effective for sequential data, such as audio signals or text sequences. After feature extraction, the output is passed through a final dense

https://doi.org/10.1021/acsomega.4c11078
ACS Omega 2025, 10, 11296−11311

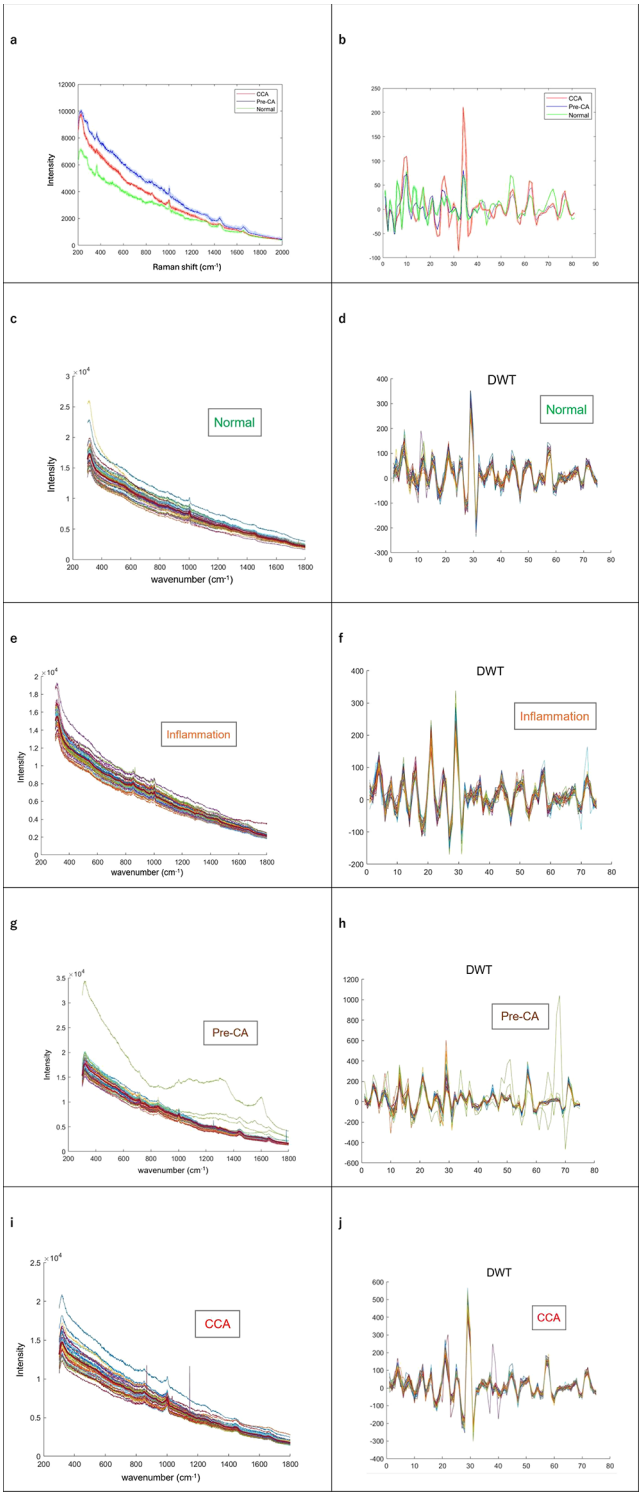

Figure 4. (a) SERS signals showing almost indiscriminable by eyes. Averaged spectrum shown and while shading represents variations. (b) the corresponding wavelet transformed signal clearly discriminate CCA signals from normal and intermediate state. Note that baseline subtraction and noise filtering were applied to SERS spectra before entering the discrete wavelet transform. (c, e, g, and (i) SERS spectra of normal, inflammation, pre-CA, and CCA respectively (49 measurements for each). (d, f, h, and j) DWT signals corresponding to the SERS in subfigures c, e, g, and i, respectively. Note that 4f and 4g can showed two outliers which can be clearly seen and excluded from both SERS and DWT where 4f (SERS) where they are more clearly discriminable between outliers and inliers. We can keep the outliers for DWT + 2D CNN method since the outliers can be excluded using regularization (L1/L2) and dropout processes within CNN.

layer, which classifies the input into four CCA stages: normal, inflammation, Pre-CA, and CCA.

2.5.2. 2D Convolutional Neural Network for CCA Stage Classification. The structure of the 2D Convolutional Neural Network (2D CNN) used for image classification is detailed in Figure 5b. The network processes input images of size 240 × 240 × 3, where the dimensions represent height, width, and the three RGB color channels, respectively. The network architecture begins with a 2D convolutional layer that applies a set of filters to the input image, extracting crucial spatial features across the image. This is followed by a max pooling layer, which reduces the dimensionality of the resulting feature maps, effectively condensing the spatial information while retaining the most significant features. The process is repeated with another convolutional and max pooling layer pair, further refining the feature maps. The refined feature maps are then flattened into a one-dimensional vector, which is passed through a fully connected hidden layer to enable more complex feature interactions. The final output layer classifies the input image into one of the predetermined classes, based on the learned features from the previous layers. This architecture effectively captures and processes the spatial hierarchies within the input images, facilitating accurate image classification.

2.5.2.1. Input Data Preparation. The classification of cholangiocarcinoma (CCA) stages, including Normal, Inflammation, Pre-CA, and CCA, is achieved by using a 2D Convolutional Neural Network (CNN) applied to images derived from the discrete wavelet transform (DWT) of one-dimensional biomedical signals. There are 2,205 data sets which are RGB images of 240 × 240 pixels. Initially, 10-fold cross-validation was used to enhance validation robustness for the limited data set. However, recognizing the increased computational demand and potential overfitting risks with CNNs, we revised our approach to a 70:30 train-test split, with data augmentation applied to the training set. Data augmentation, involving random rotations and intensity adjustments, was introduced to improve generalization and mitigate overfitting. The steps involved in the data preparation and network implementation are outlined below:

1. Signal Acquisition and Preprocessing: Biosamples and data collection were explained in previous sections. These signals are subjected to preprocessing steps such as noise reduction and normalization, to ensure the quality of the input data. The cleaned signals form the basis for the subsequent transformation.
2. Discrete Wavelet Transform (DWT): The preprocessed signals are then transformed into the time-frequency domain using DWT. The DWT provides a multi-resolution analysis of the signal, decomposing it into different frequency components while preserving temporal information. For each signal, the DWT coefficients are computed at various scales, resulting in a two-dimensional representation of the original one-dimensional signal.
3. DWT Image Generation: The DWT coefficients obtained in the previous step are arranged into a 2D

https://doi.org/10.1021/acsomega.4c11078
ACS Omega 2025, 10, 11296−11311

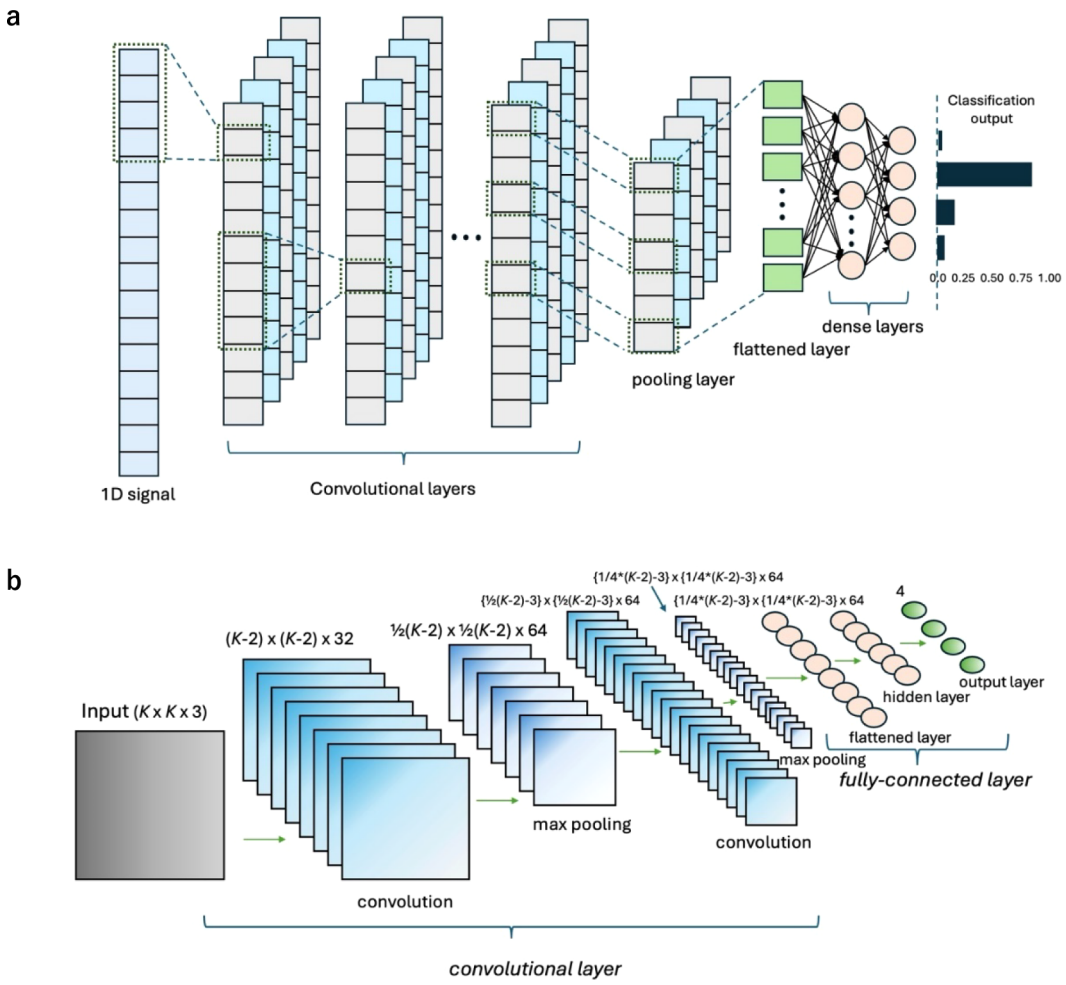

Figure 5. (a) Structure of a 1D CNN for 1D signal classification. The signal can be either raw Raman signal or feature extracted such as wavelet transformed signal. The network begins with a 1D vector signal input, followed by 8 convolutional layers that applies 1D filters to extract local features from the sequence. This is followed by a pooling layer that reduces the dimensionality of the feature maps, retaining the most significant information. The feature maps are then flattened into a one-dimensional vector, which is fed into a dense layer to process through the classification outcome, indicating the predicted class of the input sequence. (b) Structure of a 2D CNN for image classification. Input DWT image size was 240 × 240 × 3 (K = 240 in the figure; '3' corresponds to RGB). The network begins with a 2D image input, followed by a convolutional layer that applies 2D filters to extract spatial features from the image. This is followed by a max pooling layer that reduces the dimensionality of the feature maps, retaining the most significant features. Another convolutional layer and max pooling layer pair follows to further refine and condense the feature maps. The resulting feature maps are then flattened into a one-dimensional vector, which is fed into a hidden layer for additional processing. Finally, the network outputs a classification outcome, indicating the predicted class of the input image.

matrix, where each row corresponds to a specific scale, and each column corresponds to a specific time interval. We iterate DWT processing until the resolution on *x*-axis is reduced to 80 levels (but use 240 pixels for squre symmetry with vertical axis. This gives 240 × 240 × 3 RGB image for each sample, with a total number of samples is 45 × 49 = 2,205 data sets. These DWT images serve as the input to the CNN model.

2.5.2.2. 2D CNN Architecture for CCA Stage Classification. The 2D CNN architecture used for this classification task has been adapted to utilize two convolutional layers followed by max-pooling layers, culminating in a fully connected layer and an output layer. The design of the network is as follows:

1. Input Layer: The input to the network is a DWT image of a one-dimensional signal, with a shape of M × N (height M = 240, width N = 240, and 3 channels for Red-Green-Blue). Let K = M=N in Figure 5.
2. Convolutional Layer 1: This layer consists of 32 filters, each with a kernel size of 3 × 3. The activation function used is ReLU, resulting in a feature map of size $(M\text{-}2) \times (N\text{-}2) \times 32$.
3. Max-Pooling Layer 1: A pooling layer with a pool size of 2 × 2 is applied, producing a downsampled feature map of size $1/2(M\text{-}2) \times 1/2(N\text{-}2) \times 64$.
4. Convolutional Layer 2: This layer includes 64 filters with a kernel size of 3 × 3 and uses ReLU as the activation function. The output is a feature map of size $\{1/2\ (M\text{-}2)\text{-}3\} \times \{1/2(N\text{-}2)\text{-}3\} \times 64$.
5. Max-Pooling Layer 2: Another max-pooling layer with a pool size of 2 × 2 is applied, leading to a downsampled feature map of size $\{1/4(M\text{-}2)\text{-}3\} \times \{1/4(N\text{-}2)\text{-}3\} \times 64$.
6. Flatten Layer: The 3D output from the previous layer is flattened into a 1D vector of size $\{1/4(M\text{-}2)\text{-}3\} \times \{1/4(N\text{-}2)\text{-}3\} \times 64$.
7. Fully Connected Layer: This layer contains 128 units with ReLU as the activation function.

https://doi.org/10.1021/acsomega.4c11078
ACS Omega 2025, 10, 11296−11311

8. Output Layer: The final output layer has 4 units corresponding to the four classes: Normal, Inflammation, Pre-CA, and CCA, using the Softmax activation function.

The architecture provides a balanced trade-off between complexity and performance, ensuring effective feature extraction while minimizing computational cost. The use of two convolutional layers with max-pooling effectively reduces the dimensionality of the input data, capturing essential features that contribute to the classification task.

2.5.2.3. Training Process.

- Train-Test Split (70:30 Ratio): The data set is first split into training and test sets using an 70:30 ratio. This ensures that 70% of the data is used for model training, while the remaining 30% is reserved for final model evaluation.
- 10-Fold Cross-Validation: To further validate the model's performance and ensure its robustness, 10-fold cross-validation is applied on the training set. The training data is divided into ten equal-sized subsets. The model is trained and validated ten times, each time using nine subsets for training and one subset for validation. This process is repeated until each subset has been used once as the validation set. The final performance metrics are averaged over the ten iterations, providing a more reliable estimate of the model's performance.
- Loss Function and Optimization: The categorical cross-entropy loss function is used to measure the discrepancy between the predicted and actual class labels. The model is trained using an optimizer such as Adam, which adjusts the network's weights to minimize the loss function.
- Regularization and Early Stopping: Techniques such as dropout and L2 regularization are applied to prevent overfitting. Additionally, early stopping is used during training to halt the process if the validation loss stops improving, ensuring that the model generalizes well to unseen data.

We increased the number of epochs and data augmentation to avoid overfitting in the applied k-fold cross validation.[37−39] Finally, we evaluate performance of the trained 2D CNN is evaluated on the test set using metrics such as accuracy, precision, recall, and F1-score. Confusion matrices are also generated to assess the model's classification performance for each CCA stage. The results from the 10-fold cross-validation are reported, providing insights into the model's consistency and generalization across different subsets of the data. This 2D CNN-based approach utilizes the time-frequency characteristics of DWT images to achieve robust classification of CCA stages. Details will be reported in results and discussion sections. Numerical performance and resulting graphs will be in Section 3.

2.6. Mobile Application. The diagnostic tool was implemented on a mobile application platform (Figure 6), enhancing its accessibility and ease of use across various clinical settings. This mobile application allows healthcare professionals to upload SERS or Raman images directly from their devices. Once the image is uploaded, the backend system processes the data using Discrete Wavelet Transform to extract relevant features. These features are then fed into a pretrained 2D-CNN for analysis. The 2D-CNN classifies the images into one of four stages: normal, cholangitis, precancerous, or cholangiocarcinoma (CCA). This streamlined process provides quick and reliable diagnostic results, facilitating timely and accurate clinical decision-making. By exploiting the power of mobile technology, this tool has the potential to significantly improve the efficiency and accessibility of diagnosing and monitoring CCA, especially in remote or resource-limited environments. CCA stage classification result was returned after input Raman signal image was uploaded to the app.

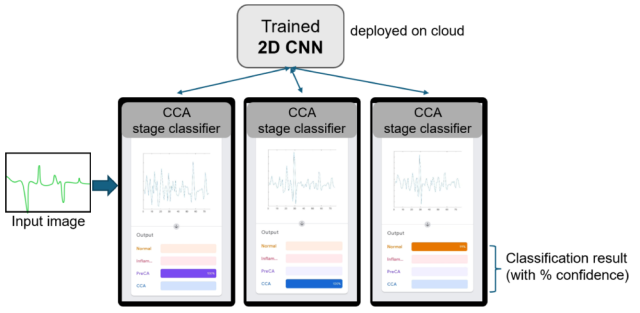

Figure 6. Mobile application interface for inputting SERS or Raman images. The backend processes these images using DWT and 2D-CNN to classify the results into four stages: normal, cholangitis, precancerous, and cholangiocarcinoma (CCA).

Details on hardware implemented, we trained our model on a high-performance computing system equipped with an NVIDIA A100 GPU, 80 GB of RAM, and an Intel Xeon processor, which provided the computational resources required to efficiently handle large data sets and complex computations. For deployment, the model was further optimized to run on mobile devices with midrange hardware specifications (e.g., devices featuring at least 4 GB of RAM and a quad-core processor). This ensures that the proposed solution is accessible to a broader user base. In addition, we address potential limitations, such as the need for periodic model updates to maintain accuracy and the compatibility challenges posed by older or lower-end devices, thereby underscoring the practical considerations and future directions for expanding the system's applicability.

3. RESULTS

The integration of SERS, wavelet transform, and CNN resulted in a robust diagnostic tool. The mobile application demonstrated high accuracy in detecting and differentiating between cholangitis, early stage CCA, CCA, and normal conditions. The integration of discrete wavelet transform (DWT) with a 2D convolutional neural network (CNN) yielded consistent classification metrics (AUC, accuracy, precision, sensitivity and F1 score) compared with other methods.

3.1. Performance Comparison. The receiver operating characteristic (ROC) curves were compared, revealing that the wavelet+CNN method exhibited the highest performance, achieving best Area Under Curve (AUC) performance. In contrast, the PCA+SVM approach demonstrated lower AUC metric. An overall comparison of various methods, including DWT+CNN, Linear Discriminant Analysis (LDA), Support Vector Machine (SVM), Artificial Neural Network (ANN), and PCA+SVM, is illustrated Figure 7, highlighting the superior efficacy of the DWT + 2D CNN technique over the other methods.

The ROC curves and AUC values indicate that the DWT + 2D CNN method outperforms other methods in terms of

https://doi.org/10.1021/acsomega.4c11078
ACS Omega 2025, 10, 11296−11311

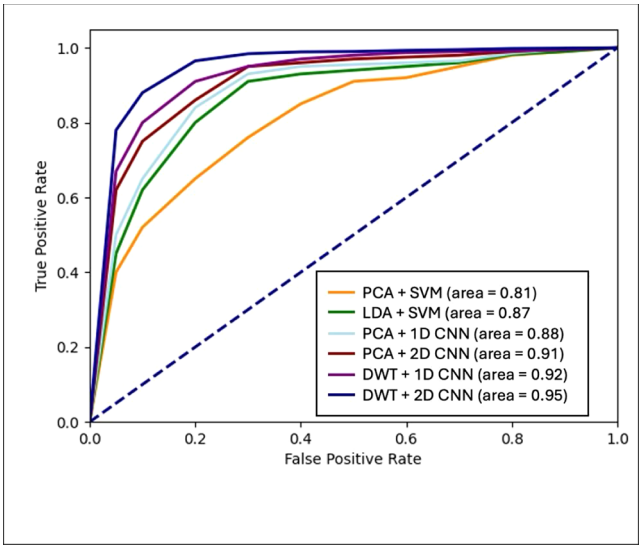

Figure 7. ROC curves illustrating the performance comparison of various classification models. The DWT + 2D CNN model achieved an AUC of 0.95, while the DWT + 1D CNN model yielded an AUC of 0.92. The PCA + 2D CNN model attained an AUC of 0.91, and the PCA + 1D CNN model reached an AUC of 0.88. Additionally, the LDA + SVM model achieved an AUC of 0.87, and the PCA + SVM model obtained an AUC of 0.81.

accuracy and robustness, making it the most effective approach for classifying SERS spectra in this study. However, the choice of method should consider the trade-offs between complexity, computational resources, and performance requirements.

From the confusion matrices (Figure 8), we computed the overall performance as follows. The combination of wavelet

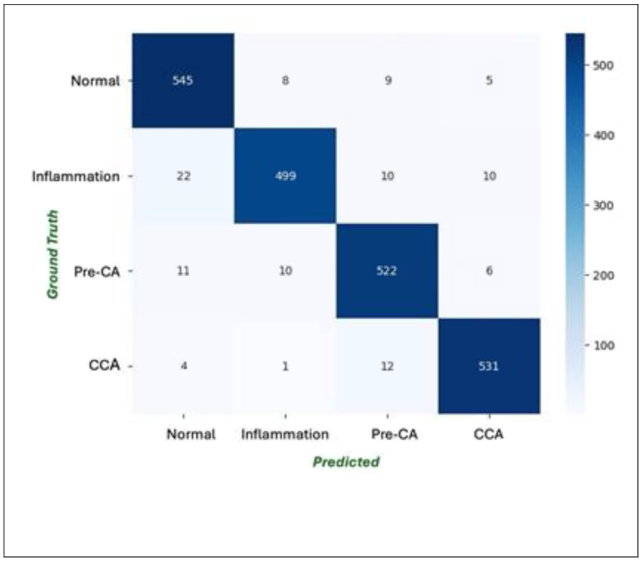

Figure 8. Confusion matrices of each signal processing and machine learning methods.

transform and 2D CNN resulted in superior performance metrics surpassing those obtained using principal component analysis (PCA) or linear discriminant analysis (LDA) combined with CNN methods. The data set consisted of serum samples from 50 hamsters, with each serum subjected to 49 SERS measurements thus giving 49× larger data sets to ensure that data sets are sufficient to be trained and that outliers can be rejected automatically. To ensure robust evaluation, a 10-fold cross-validation approach was employed.

The overall performance comparison of different methods was shown in Table 1. According to Table 1, the comparison

Table 1. Accuracy, Precision, Recall and F1 Score Comparison Between Different Approaches

Method	Accuracy (%)	Sensitivity (Recall) (%)	Specificity (%)	F1 Score (%)
DWT + 2D CNN	95.10	95.08	98.36	95.10
DWT + 1D CNN	92.00	91.50	96.00	91.75
PCA + 1D CNN	88.00	87.50	94.00	87.75
LDA + SVM	84.50	84.00	90.50	84.25
PCA + SVM	82.40	82.00	88.40	82.20

of classifier performance metrics reveals significant insights into the efficacy of various methods in the classification of CCA stages (normal, inflamed, Pre-CA, and CCA). The DWT + 2D CNN method emerged as the superior approach, achieving the highest accuracy of 95.10%, sensitivity (recall) of 95.08%, specificity of 98.36%, and F1 score of 95.10%. These metrics underscore the method's exceptional capability in distinguishing between the various stages of CCA with high precision and reliability. In contrast, the DWT + 1D CNN method, while still performing robustly, showed slightly lower performance with an accuracy of 92.00%, sensitivity of 91.50%, specificity of 96.00%, and F1 score of 91.75%. The superior performance of DWT + 1D CNN over PCA + 1D CNN, which achieved an accuracy of 88.00%, sensitivity of 87.50%, specificity of 94.00%, and F1 score of 87.75%, can be attributed to the nature of the whole Raman spectra. Raman spectra are nonlinear and thus require nonlinear feature extraction methods like the discrete wavelet transform (DWT). DWT efficiently captures all the Raman shifts and is more effective in extracting features from nonlinear data sets compared to PCA and LDA, which are linear methods.

4. DISCUSSION

In this study, we evaluated various machine learning techniques for early detection of Cholangiocarcinoma (CCA) using Surface-Enhanced Raman Scattering (SERS) spectra. We compared 2D Convolutional Neural Network (2D CNN) combined with Discrete Wavelet Transform (DWT) against Principal Component Analysis with Support Vector Machine (PCA + SVM), Linear Discriminant Analysis with SVM (LDA + SVM), PCA with 1D CNN (PCA + 1D CNN), PCA with 2D CNN (PCA + 2D CNN), and DWT with 1D CNN (DWT + 1D CNN). Our results showed that the DWT + 2D CNN approach significantly outperformed as summarized in Figure 8 and Table 1. The introduction of wavelet transform to the SERS signal processing significantly improved the discrimination performance, enhancing the tool's overall diagnostic capability. We increase the number of epochs to prevent overfitting risk when we use 10-fold cross validation.

Further down the performance scale, the PCA + 1D CNN method demonstrates the utility of principal component analysis (PCA) in dimensionality reduction and the efficacy of 1D CNNs, though the performance is not as high as methods incorporating wavelet transforms. The LDA + SVM and PCA + SVM methods, with accuracies of 84.50% and 82.40% respectively, show the potential of linear discriminant

https://doi.org/10.1021/acsomega.4c11078
ACS Omega 2025, 10, 11296−11311

analysis (LDA) and PCA combined with support vector machines (SVM). However, their lower sensitivity and specificity indicate that these methods may struggle with the more nuanced distinctions between CCA stages compared to the CNN-based approaches. Overall, the results highlight the superiority of the DWT + 2D CNN method for CCA stage classification, suggesting that the combination of wavelet-based feature extraction with deep learning models provides a powerful framework for medical image classification tasks. The high specificity of 98.36% is particularly noteworthy, indicating a strong ability to correctly identify non-CCA stages, which is crucial for reducing false positives in clinical settings. In this study, the whole Raman or SERS shifts were feature-extracted efficiently by DWT, demonstrating its superior capability in handling the inherent nonlinearity of the data.

PCA and LDA, being linear methods, are limited in their ability to handle the nonlinear classification required for complex SERS spectra. These methods often rely on peak sampling, which can miss critical information hidden in the full Raman spectra. In contrast, DWT captures the entire Raman wavelength range, enabling it to extract features from previously unrecognized signals. This comprehensive feature extraction is further refined by the 2D CNN, which excels in learning hierarchical patterns, leading to high-performance classification of CCA stages. The DWT+2D CNN combination thus achieves the best performance in this study.

Additional discussion on preprocession steps, the contribution of ALS baseline correction and Savitzky-Golay filtering was assessed by comparing classification accuracy with and without these preprocessing steps. Without any preprocessing, using the same feature extraction and ML model (DWT + 2D CNN), the model achieved 88.2% accuracy; when these methods were applied, accuracy increased to 95.1%, highlighting the importance of effective baseline correction and noise reduction in enhancing overall model performance.

Overall, this research introduces an advanced method for early CCA detection by leveraging SERS for high sensitivity, DWT for thorough feature extraction, and 2D CNN for robust pattern recognition. The development of a mobile application based on this approach offers an accurate and accessible tool for early diagnosis, potentially improving patient outcomes.

4.1. Comparative Performance Analysis. *4.1.1. Accuracy and Robustness.* The accuracy of the DWT+2D CNN model was consistently higher than that of PCA+SVM, LDA +SVM, PCA+1D CNN, PCA+2D CNN, and DWT+1D CNN. This indicates a superior ability to accurately (95%) classify CCA, pre-CA, inflammation and normal stages from serum. The 2D CNN's capability to capture intricate patterns in the SERS spectra, combined with the multiresolution analysis provided by the DWT, contributes to its enhanced performance. Unlike PCA and LDA, which are linear methods and struggle with nonlinear separable data sets, the DWT+2D CNN model effectively resolves the nonlinear separable nature of SERS spectra. PCA and LDA reduce dimensionality linearly, often leading to overlapping data points in complex data sets, while DWT captures both time and frequency information, and 2D CNN processes these features hierarchically, enhancing the model's ability to discern subtle differences in the data.

4.1.2. Sensitivity, Specificity and Precision. Sensitivity (recall) and specificity are critical metrics for assessing the model's performance in detecting CCA cases and avoiding false positives. The DWT+2D CNN model achieved higher sensitivity and specificity compared to the other methods. This suggests that our model is more adept at identifying true positive cases of CCA and reducing false positive rates, thereby providing a reliable tool for early detection, and minimizing unnecessary diagnostic procedures. The multiresolution feature of DWT, combined with the deep learning capabilities of 2D CNN, enables the model to capture intricate patterns that are indicative of CCA, which are often missed by linear methods like PCA and LDA.

Precision, which measures the proportion of true positive predictions, was also higher for the DWT+2D CNN model. This high precision indicates fewer false positive predictions, which is crucial in clinical settings to avoid unnecessary anxiety and treatment for patients. The F1 score, representing the harmonic mean of precision and recall, further confirmed the balanced performance of the DWT+2D CNN model. This balance is essential for ensuring that the model is reliable and effective in practical applications. The nonlinear processing capability of DWT combined with the hierarchical feature learning of 2D CNN results in a more nuanced and accurate classification.

4.1.3. ROC and AUC. The ROC curve and AUC provide a comprehensive measure of the model's performance across different threshold values. The DWT+2D CNN model demonstrated a more favorable ROC curve and a significantly higher AUC compared to PCA + SVM, LDA + SVM, PCA + 1D CNN, PCA + 2D CNN, and DWT + 1D CNN. A higher AUC indicates better overall discriminative ability, reinforcing the superior performance of our model in distinguishing between CCA and non-CCA cases. The ability of DWT to handle nonstationary signals and the deep learning power of 2D CNN contribute to this enhanced performance, which linear methods cannot achieve due to their inherent limitations with nonlinear data sets.

4.2. Advantages and Limitations of the Proposed DWT + 2D CNN. *4.2.1. Advantages.* The DWT+2D CNN approach offers several distinct advantages in the early detection of CCA using SERS spectra. First, the Discrete Wavelet Transform (DWT) is particularly effective in capturing both time and frequency information from the SERS spectra, resulting in a comprehensive and rich feature set that is crucial for accurate analysis. Unlike traditional peak sampling methods, which might miss critical information related to biomolecules by focusing only on specific spectral peaks, DWT considers the entire spectra, ensuring that no potentially important data is overlooked. This holistic approach allows the model to retain essential signal characteristics at various scales, which is invaluable for detecting the complex biochemical signatures of early stage CCA. Second, the deep learning capabilities of the 2D Convolutional Neural Network (CNN) further enhance this approach. The 2D CNN excels at learning hierarchical features from the input data, enabling it to identify and distinguish subtle patterns and anomalies that might be indicative of early stage CCA. This hierarchical feature learning is critical for capturing intricate relationships within the data that simpler models might miss. Moreover, the robustness of the DWT+2D CNN approach is a significant advantage. This combined method is highly resilient to variations and noise within the SERS data, which is often encountered in real-world clinical settings. This robustness ensures that the model maintains high performance and reliability across diverse data sets and conditions, making it a dependable tool for early detection of CCA. Additionally, the

https://doi.org/10.1021/acsomega.4c11078
ACS Omega 2025, 10, 11296−11311

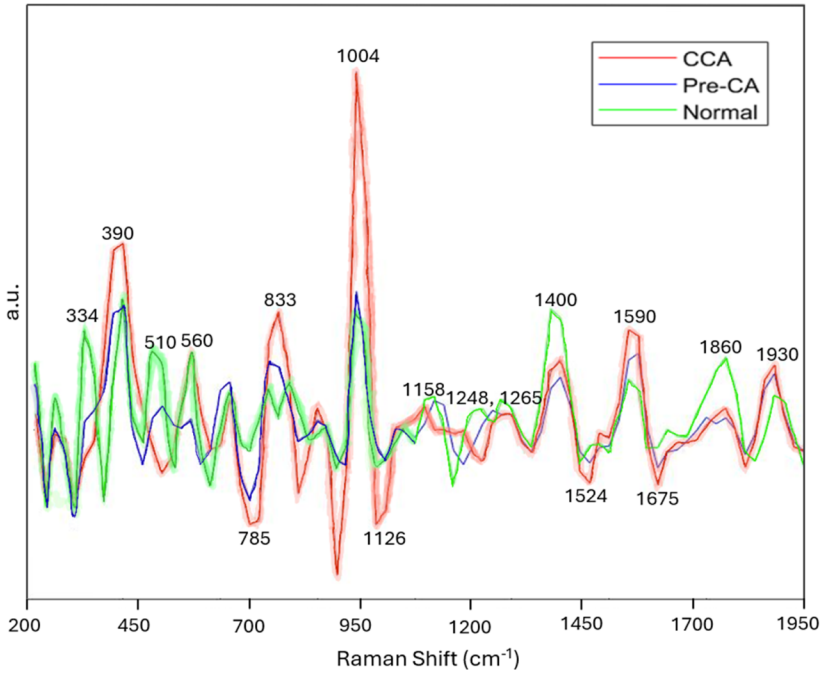

Figure 9. Peak Associations after wavelet upsampling to the original scale of SERS spectrum. Significant peaks to identify the difference between normal, precancerous, and CCA were labeled.

integration of DWT with a 2D CNN synergize the strengths of both techniques, resulting in the boost of overall model accuracy, sensitivity, specificity, and AUC performance. This study showed that DWT + 2D CNN can promisingly be a superior method for early detection of CCA, potentially leading to improved patient outcomes through earlier and more accurate diagnosis.

4.2.2. Limitations and Challenges. Despite the advantages of the DWT+2D CNN approach for early detection of CCA using SERS spectra, several limitations and challenges need to be addressed. One primary concern is the computational complexity associated with this model. The DWT+2D CNN requires significant computational resources for both training and signal processing, which may restrict its applicability in resource-constrained environments, such as smaller medical facilities or regions with limited access to advanced computational infrastructure. However, current computing technology could compute the required discrete wavelet transform and 2D CNNs in a few seconds.

Additionally, the performance of deep learning models, including the DWT+2D CNN, is highly dependent on the quality and quantity of the training data. Ensuring a diverse and representative data set is crucial for the model's generalizability and robustness. However, acquiring large, annotated data sets of SERS spectra from CCA patients can be challenging, given the rarity of the disease. This data dependency can lead to overfitting, where the model performs well on the training data but fails to generalize to new, unseen data, limiting its clinical utility.

Another challenge is the interpretability of the DWT+2D CNN model. While the model provides high accuracy, clinicians may require additional tools to understand and trust the model's predictions. Techniques such as saliency maps, which highlight the regions of the input data that most influence the model's decision, can provide insights into the model's reasoning, helping clinicians understand and trust the automated predictions.

Furthermore, integrating advanced models into existing clinical workflows presents its own set of challenges. The need for specialized software and hardware, along with training for medical personnel to operate these systems effectively, adds layers of complexity to their deployment. Addressing these limitations through continuous research, development of interpretability techniques, and collaboration with clinical experts is vital for the successful integration of the DWT+2D CNN approach in real-world healthcare settings. Only then can the full potential of this powerful diagnostic tool be realized, leading to earlier detection and better outcomes for CCA patients.

4.3. Peak Associations. Raman spectral analysis for cholangiocarcinoma (CCA) detection offers a detailed molecular fingerprint by associating specific vibrational peaks with distinct chemical bonds and biochemical components. For instance, in Figure 9, the 1004 cm^{-1} band arises from the C−C ring breathing of phenylalanine, a marker for protein composition and structural integrity. At 1158 cm^{-1}, the observed C−C stretching is attributed to β-carotene, serving as an indicator of oxidative stress within the cellular environment. The peaks at 1248 cm^{-1} and 1265 cm^{-1} correspond to the Amide III bands, which involve C−N stretching and N−H bending in peptide bonds, reflecting alterations in protein secondary structures such as β-sheets. The 1675 cm^{-1} band, linked to C═O stretching in the Amide I region, further underscores changes in the α-helix conformation, highlighting protein folding variations associated with disease progression.

Additional significant peaks provide further insights into the biochemical landscape. The 560 cm^{-1} peak, corresponding to S−S stretching in disulfide bonds, indicates modifications in protein folding and stability. The 785 cm^{-1} band, due to C−H bending in aromatic rings, and the 833 cm^{-1} band, linked to

https://doi.org/10.1021/acsomega.4c11078
ACS Omega 2025, 10, 11296−11311

C−H bending in protein aromatic side chains, both suggest alterations in the structures of nucleic acids and proteins. At 1126 cm^{-1}, the C−N stretching mode further delineates changes in peptide bonds and overall protein structure. The 1400 cm^{-1} band, characterized by CH_2 bending, is indicative of interactions between lipids and proteins that may be disrupted in cancerous cells. Moreover, the 1524 cm^{-1} and 1590 cm^{-1} bands, which stem from C═C stretching in unsaturated lipids and aromatic amino acids respectively, point to perturbations in lipid metabolism and protein conformation. Finally, the peaks at 1860 cm^{-1} and 1930 cm^{-1}, arising from C═O stretching in aldehydes and anhydrides, serve as markers for lipid oxidation, a process closely linked with the tumor microenvironment.

By directly correlating these Raman shifts with their respective chemical bonds, the analysis provides a robust framework for understanding the molecular changes associated with CCA formation. However, sampling discrete peaks may be insufficient to cover all hidden information about other compounds. Therefore, this work proposed using whole spectrum with near-lossless compression using DWT.

Integrating the SERS spectrum in our proposed DWT across the entire spectral range ensures efficient data handling while preserving essential spectral details. When integrated with a 2D Convolutional Neural Network (2D CNN), this approach enables robust and highly accurate stage classification of CCA from blood serum, offering a promising framework for early cancer detection, disease progression monitoring, and potential clinical applications.

4.4. Comparison with Related Studies. Compared with previous Raman spectroscopy-based methods for CCA diagnosis (Table 2), which often focused primarily on binary classification (either distinguishing CCA from healthy serum or separating cholangitis from CCA) and faced constraints such as small sample size, tissue heterogeneity, and limited spectral signal, this work (Study 4) introduces a novel approach by integrating Surface-Enhanced Raman Spectroscopy (SERS) with Discrete Wavelet Transform (DWT) and a two-dimensional Convolutional Neural Network (2D CNN). While the earlier studies demonstrated promising sensitivity and specificity in differentiating CCA from healthy or inflamed serum samples, they often required larger patient cohorts or multiple spectra acquisitions to overcome spectral variability and ensure reliability. In contrast, the present study effectively addresses these challenges by employing an enhanced Raman signal (via SERS) and advanced machine learning techniques (DWT + 2D CNN) to classify four distinct stages of CCA. Although validation on human serum remains necessary for broad clinical applicability, this framework represents a significant advancement, suggesting improved diagnostic accuracy and the potential for more nuanced staging of CCA compared to the prior work.

4.5. Future Directions. Future research should focus on several key areas to enhance the DWT+2D CNN model's effectiveness for early detection of Cholangiocarcinoma (CCA). First, further optimization of the model, including hyperparameter tuning and architectural improvements, is essential to boost its performance and efficiency. Second, extensive clinical validation using larger and more diverse data sets is crucial to confirm the model's robustness and generalizability in real-world settings. Third, exploring hybrid models that combine the strengths of different machine learning techniques could lead to even better performance and

Table 2. Comparison with Related Studies

Study	Contributions	Limitations	Citation
1. Rapid Label-Free Detection of Cholangiocarcinoma from Human Serum	Demonstrated high sensitivity (86.67%) and specificity (96.67%) using Raman spectroscopy with PCA-LDA for distinguishing CCA from healthy serum.	- Small sample size (30 patients per group) may limit generalizability. - Weak signal intensity and fluorescence interference can affect clinical application. - CCA patients in the study were mostly on moderate and late stage which is infeasible for treatment.	Suksuratin et al. (2022)[28]
2. Rapid, Label-Free Histopathological Diagnosis of Liver Cancer	Showed potential for Raman spectroscopy to complement traditional imaging in liver cancer diagnosis, including CCA.	- Tissue heterogeneity complicates spectral data analysis. - Requires collection of multiple spectra for consistent accuracy, increasing complexity.	Huang et al. (2023)[40]
3. Noninvasive Cholangitis and Cholangiocarcinoma Screening Based on Serum Raman Spectroscopy	- Explored noninvasive differentiation between cholangitis and cholangiocarcinoma using serum Raman spectroscopy and support vector machines.	- Faces challenges similar to previous studies regarding sample size and spectral variability. - Requires careful validation across diverse patient populations.	Su, Dawuti and Zhao (2022)[41]
4. SERS + DWT + 2D CNN	– First report of using SERS with DWT and 2D CNN to classify 4 stages of CCA from blood serum with high sensitivity and specificity	– This study was carried out on hamster serum. Future study on human serum should be continue to validate and ensure for the practical application.	*This work*

https://doi.org/10.1021/acsomega.4c11078
ACS Omega 2025, 10, 11296−11311

robustness. Once clinical validation is complete, extending the usage of the model is imperative. We have developed a mobile application that allows users to input Raman or SERS spectra images and receive classifications of CCA stages. This application aims to make advanced diagnostic tools accessible and practical in various clinical environments, further supporting early detection and improved patient outcomes. Though it attained high classification performance, this work was conducted on hamster serum and CCA stages in hamster. Human clinical trials are still needed to be further studied and check for its reproducibility before extending its impact.

We chose a 2D CNN to enable portable Raman spectrometer and mobile application integration for future practical CCA field testing.

5. CONCLUSIONS

In this study, we demonstrated that the combination of Surface-Enhanced Raman Scattering (SERS), Discrete Wavelet Transform (DWT), and a 2D Convolutional Neural Network (2D CNN) significantly outperforms other methods for the early detection of Cholangiocarcinoma (CCA). This is also the first report of using SERS for CCA classification. Unlike linear methods such as PCA and LDA, which may miss critical information by focusing solely on spectral peaks, DWT extracts feature from the entire Raman spectrum and refines these features for superior classification of CCA stages through the 2D CNN. The 2D CNN outperforms other classification methods using SERS data due to its invariance to translation or SERS peak shifting, which can cause inconsistencies in other approaches. This method shows great promise. Integrating these technologies into a mobile application could provide a powerful, accurate, and accessible tool for the early detection of CCA, potentially improving survival rates and patient outcomes. Future research should validate these findings in larger clinical trials (in human) and explore the application of this technique to other types of cancer, thereby broadening its impact on point of care, early cancer detection and preventive care.

■ ASSOCIATED CONTENT

Data Availability Statement

The original contributions presented in this study are included in the article/Supporting Information. Further inquiries can be directed to the corresponding author(s).

Supporting Information

The Supporting Information is available free of charge at https://pubs.acs.org/doi/10.1021/acsomega.4c11078.

Video demo of the mobile app (MP4)

Averaged SERS + DWT on serum in 4 classes (CCA, inflammation, precancerous, and normal) (ZIP)

■ AUTHOR INFORMATION

Corresponding Author

Chavis Srichan − *Department of Computer Engineering, Faculty of Engineering, Khon Kaen University, Khon Kaen 40002, Thailand; Department of Biomedical Engineering, Faculty of Engineering, Khon Kaen University, Khon Kaen 40002, Thailand;* orcid.org/0000-0002-4772-3543; Email: chavis@kku.ac.th

Authors

Pobporn Danvirutai − *College of Computing, Khon Kaen University, Khon Kaen 40002, Thailand*

Thatsanapong Pongking − *Department of Parasitology, Faculty of Medicine, Khon Kaen University, Khon Kaen 40002, Thailand; Cholangiocarcinoma Research Institute, Khon Kaen University, Khon Kaen 40002, Thailand*

Suppakrit Kongsintaweesuk − *Department of Parasitology, Faculty of Medicine, Khon Kaen University, Khon Kaen 40002, Thailand; Cholangiocarcinoma Research Institute, Khon Kaen University, Khon Kaen 40002, Thailand*

Somchai Pinlaor − *Department of Parasitology, Faculty of Medicine, Khon Kaen University, Khon Kaen 40002, Thailand; Cholangiocarcinoma Research Institute, Khon Kaen University, Khon Kaen 40002, Thailand;* orcid.org/0000-0002-8187-7247

Sartra Wongthanavasu − *College of Computing, Khon Kaen University, Khon Kaen 40002, Thailand*

Complete contact information is available at: https://pubs.acs.org/10.1021/acsomega.4c11078

Author Contributions

Formal analysis, Investigation, Methodology, Writing−original draft, P.D.; Resources, Investigation, Data Curation, Validation, T.P.; Resources, Investigation, Data Curation, Validation, S.K.; Investigation, Data Curation, Validation, Funding acquisition, Project Administration, S.P.; Formal analysis, Conceptualization, Supervision, S.W.; Analysis, Conceptualization, Methodology, Visualization, Project Administration, Writing−original draft, Writing−review and editing, C.S.

Funding

This research is funded by NICT Japan under ASEAN IVO 2023 Project "Innovation of Photonic and Electrochemical Biosensors for Cholangiocarcinoma Diagnosis".

Notes

The study protocol (IACUC-KKU-56/66) underwent scrutiny by Khon Kaen University's Animal Ethics Committee in accordance with the ethical guidelines for the use of animals in experiments described by National Research Council, Thailand.

The authors declare no competing financial interest.

■ ACKNOWLEDGMENTS

We acknowledge the funding support from NICT, Japan, under the ASEAN IVO 2023 Project, "Innovation of Photonic and Electrochemical Biosensors for Cholangiocarcinoma Diagnosis." We greatly acknowledge the histological assistance from Prof. Chawalit Pairojkul. Special thanks are extended to Dr. Sirinapa Klungsaeng for her contributions during the initial phase of this work. Collaborations with NECTEC team through Dr. Pitak Eiamchai and Dr. Mati Horprathum are greatly appreciated.

■ REFERENCES

(1) Van der Gaag, N. A.; Kloek, J. J.; de Bakker, J. K. Survival analysis and prognostic nomogram for patients undergoing resection of extrahepatic cholangiocarcinoma. *Ann. Oncol.* **2012**, *23*, 2642−2649.

(2) Qurashi, M.; Vithayathil, M.; Khan, S. A. Epidemiology of cholangiocarcinoma. *Eur. J. Surg. Oncol.* **2025**, *51* (2), 107064.

(3) Pascale, A.; Rosmorduc, O.; Duclos-Vallée, J. C. New epidemiologic trends in cholangiocarcinoma. *Clin. Res. Hepatol. Gastroenterol.* **2023**, *47* (9), 102223.

(4) Sithithaworn, P.; Yongvanit, P.; Duenngai, K.; Kiatsopit, N.; Pairojkul, C. Roles of liver fluke infection as risk factor for cholangiocarcinoma. *J. Hepatobiliary Pancreat. Sci.* **2014**, *21*, 301−308.
(5) Tyson, G. L.; El-Serag, H. B. Risk factors for cholangiocarcinoma. *Hepatology* **2011**, *54*, 173−184.
(6) Khan, S. A.; Davidson, B. R.; Goldin, R. D.; Heaton, N.; Karani, J.; Pereira, S. P.; Wasan, H. Guidelines for the diagnosis and treatment of cholangiocarcinoma: an update. *Gut* **2012**, *61*, 1657−1669.
(7) Buerlein, R. C.; Wang, A. Y. Endoscopic retrograde cholangiopancreatography-guided ablation for cholangiocarcinoma. *Gastrointest. Endosc. Clin.* **2019**, *29*, 351−367.
(8) Turan, A. S.; Jenniskens, S.; Martens, J. M.; Rutten, M. J.; Yo, L. S.; van Strijen, M. J.; van Geenen, E. J. Complications of percutaneous transhepatic cholangiography and biliary drainage, a multicenter observational study. *Abdom. Radiol.* **2022**, *47*, 3338−3344.
(9) Ilyas, S. I.; Gores, G. J. Pathogenesis, diagnosis, and management of cholangiocarcinoma. *Gastroenterology* **2013**, *145*, 1215−1229.
(10) DeOliveira, M. L.; Cunningham, S. C.; Cameron, J. L. Cholangiocarcinoma: thirty-one-year experience with 564 patients at a single institution. *Ann. Surg.* **2007**, *245*, 755−762.
(11) Lee, T.; Teng, T. Z. J.; Shelat, V. G. Carbohydrate Antigen 19−9—Tumor Marker: Past, Present, and Future. *World J. Gastrointest. Surg.* **2020**, *12* (12), 468−490.
(12) Zhang, J.; Qin, S. D.; Li, Y.; Lu, F.; Gong, W. F.; Zhong, J. H.; De Xiang, B.; Zhao, J. F.; Zhan, G. H.; Li, P. Z.; Song, B.; De Xiang, B. Prognostic significance of combined α-fetoprotein and CA19-9 for hepatocellular carcinoma after hepatectomy. *World J. Surg Oncol.* **2022**, *20* (1), 346.
(13) Rizzo, A.; Ricci, A. D.; Tavolari, S.; Brandi, G. Circulating Tumor DNA in Biliary Tract Cancer: Current Evidence and Future Perspectives. *Cancer Genomics Proteomics* **2020**, *17* (5), 441−452.
(14) Salem, P. E. S.; Ghazala, R. A.; El Gendi, A. M. E.; Emara, D. M.; Ahmed, N. M. The Association Between Circulating MicroRNA-150 Level and Cholangiocarcinoma. *J. Clin. Lab. Anal.* **2020**, *34* (11), No. e23397.
(15) Saengboonmee, C.; Sawanyawisuth, K.; Chamgramol, Y.; Wongkham, S. Prognostic Biomarkers for Cholangiocarcinoma and Their Clinical Implications. *Expert Rev. Anticancer Ther.* **2018**, *18* (6), 579−592.
(16) Vázquez-Iglesias, L.; Casagrande, G. M. S.; García-Lojo, D.; Leal, L. F.; Ngo, T. A.; Pérez-Juste, J.; Reis, R. M.; Kant, K.; Pastoriza-Santos, I. SERS Sensing for Cancer Biomarker: Approaches and Directions. *Bioact. Mater.* **2024**, *34*, 248−268.
(17) Murali, V. P.; Karunakaran, V.; Murali, M.; Lekshmi, A.; Kottarathil, S.; Deepika, S.; Maiti, K. K.; Ramya, A. N.; Raghu, K. G.; Sujathan, K.; Maiti, K. K. A Clinically Feasible Diagnostic Spectro-Histology Built on SERS-Nanotags for Multiplex Detection and Grading of Breast Cancer Biomarkers. *Biosens. Bioelectron.* **2023**, *227*, 115177.
(18) Iancu, S. D.; Cozan, R. G.; Stefancu, A.; David, M.; Moisoiu, T.; Moroz-Dubenco, C.; Leopold, N.; Chira, C.; Andreica, A.; Leopold, L. F.; Eniu, D. T.; et al. SERS Liquid Biopsy in Breast Cancer: What Can We Learn from SERS on Serum and Urine? *Spectrochim. Acta, Part A* **2022**, *273*, 120992.
(19) Choi, N.; Dang, H.; Das, A.; Sim, M. S.; Chung, I. Y.; Choo, J. SERS Biosensors for Ultrasensitive Detection of Multiple Biomarkers Expressed in Cancer Cells. *Biosens. Bioelectron.* **2020**, *164*, 112326.
(20) Huang, Y.; Xie, T.; Zou, K.; Gu, Y.; Yang, G.; Zhang, F.; Yang, S.; Yang, S. Ultrasensitive SERS Detection of Exhaled Biomarkers of Lung Cancer Using a Multifunctional Solid Phase Extraction Membrane. *Nanoscale* **2021**, *13* (31), 13344−13352.
(21) Zhang, J.; Dong, Y.; Zhu, W.; Xie, D.; Zhao, Y.; Yang, D.; Li, M. Ultrasensitive Detection of Circulating Tumor DNA of Lung Cancer via an Enzymatically Amplified SERS-Based Frequency Shift Assay. *ACS Appl. Mater. Interfaces* **2019**, *11* (20), 18145−18152.
(22) Haroon, M.; Tahir, M.; Nawaz, H.; Majeed, M. I.; Al-Saadi, A. A. Surface-Enhanced Raman Scattering(SERS) Spectroscopy for Prostate Cancer Diagnosis: A Review. *Photodiagn. Photodyn. Ther.* **2022**, *37*, 102690.
(23) Zhao, J.; Wang, J.; Liu, Y.; Han, X. X.; Xu, B.; Ozaki, Y.; Zhao, B. Detection of Prostate Cancer Biomarkers via a SERS-Based Aptasensor. *Biosens. Bioelectron.* **2022**, *216*, 114660.
(24) Gurian, E.; Di Silvestre, A.; Mitri, E.; Pascut, D.; Tiribelli, C.; Giuffrè, M.; Crocè, L. S.; Sergo, V.; Bonifacio, A. Repeated Double Cross-Validation Applied to the PCA-LDA Classification of SERS Spectra: A Case Study with Serum Samples from Hepatocellular Carcinoma Patients. *Anal. Bioanal. Chem.* **2021**, *413* (5), 1303−1312.
(25) Wu, J.; Zhou, X.; Li, P.; Lin, X.; Wang, J.; Hu, Z.; Zhang, P.; Chen, D.; Cai, H.; Niessner, R.; et al. Ultrasensitive and Simultaneous SERS Detection of Multiplex MicroRNA Using Fractal Gold Nanotags for Early Diagnosis and Prognosis of Hepatocellular Carcinoma. *Anal. Chem.* **2021**, *93* (25), 8799−8809.
(26) Managò, S.; Tramontano, C.; Cave, D. D.; Chianese, G.; Zito, G.; De Stefano, L.; Rea, I.; Lonardo, E.; De Luca, A. C.; Rea, I. SERS Quantification of Galunisertib Delivery in Colorectal Cancer Cells by Plasmonic-Assisted Diatomite Nanoparticles. *Small* **2021**, *17* (34), 2101711.
(27) Peng, S.; Lu, D.; Zhang, B.; You, R.; Chen, J.; Xu, H.; Lu, Y. Machine Learning−Assisted Internal Standard Calibration Label-Free SERS Strategy for Colon Cancer Detection. *Anal. Bioanal. Chem.* **2023**, *415* (9), 1699−1707.
(28) Suksuratin, P.; Rodpai, R.; Luvira, V.; Intapan, P. M.; Maleewong, W.; Chuchuen, O. Rapid Label-Free Detection of Cholangiocarcinoma from Human Serum Using Raman Spectroscopy. *PLoS One* **2022**, *17* (10), No. e0275362.
(29) Driskell, J. D.; Shanmukh, S.; Liu, Y.; Chaney, S. B.; Tang, X. J.; Zhao, Y. P.; Dluhy, R. A. The Use of Aligned Silver Nanorod Arrays Prepared by Oblique Angle Deposition as Surface Enhanced Raman Scattering Substrates. *J. Phys. Chem. C* **2008**, *112* (4), 895−901.
(30) Senapati, S.; Kaur, M.; Singh, N.; Kulkarni, S. S.; Singh, J. P. Affordable Paper-Based Surface-Enhanced Raman Scattering Substrates Containing Silver Nanorods Using Glancing-Angle Deposition for Nosocomial Infection Detection. *ACS Appl. Nano Mater.* **2024**, *7* (7), 6736−6748.
(31) LeCun, Y.; Bengio, Y.; Hinton, G. Deep Learning. *Nature* **2015**, *521*, 436−444.
(32) Cong, S.; Zhou, Y. A Review of Convolutional Neural Network Architectures and Their Optimizations. *Artif. Intell. Rev.* **2023**, *56* (3), 1905−1969.
(33) Botta, R.; Eiamchai, P.; Horprathum, M.; Limwichean, S.; Chananonnawathorn, C.; Patthanasettakul, V.; Nuntawong, N. Investigation of Silver Nanorods as Reusable SERS-Active Substrates for Trace Level Detection of 2-MIB Volatile Organic Compound. *Sens. Actuators, B* **2018**, *271*, 122−127.
(34) Zhou, Q.; Li, Z.; Yang, Y.; Zhang, Z. Arrays of Aligned, Single Crystalline Silver Nanorods for Trace Amount Detection. *J. Phys. D: appl. Phys.* **2008**, *41* (15), 152007.
(35) Zhao, Y.; Kumar, A.; Yang, Y. Unveiling Practical Considerations for Reliable and Standardized SERS Measurements: Lessons from a Comprehensive Review of Oblique Angle Deposition-Fabricated Silver Nanorod Array Substrates. *Chem. Soc. Rev.* **2024**, *53* (2), 1004−1057.
(36) Kang, Y. Design of Armrest Ag Nanorod Arrays with High SERS Performance for Sensitive Biomolecule Detection. *J. Phys. Chem. C* **2020**, *124* (38), 21054−21062.
(37) Akbar, M.; Ullah, M.; Shah, B.; Khan, R. U.; Hussain, T.; Ali, F. An Effective Deep Learning Approach for the Classification of Bacteriosis in Peach Leaves. *Front. Plant Sci.* **2022**, *13*, 1064854.
(38) Torres-Galván, J. C.; Guevara, E.; Kolosovas-Machuca, E. S.; Oceguera-Villanueva, A.; Flores, J. L.; González, F. J. Deep Convolutional Neural Networks for Classifying Breast Cancer Using Infrared Thermography. *Quant. InfraRed Thermogr. J.* **2022**, *19* (4), 283−294.
(39) Esteva, A.; Kuprel, B.; Novoa, R. Dermatologist-Level Classification of Skin Cancer with Deep Neural Networks. *Nature* **2017**, *542*, 115−118.
(40) Huang, L.; Sun, H.; Sun, L.; Shi, K.; Chen, Y.; Ren, X.; Wang, Y. R.; Jiang, D.; Liu, X.; Knoll, W.; Zhang, Q.; Wang, Y. Label-Free

https://doi.org/10.1021/acsomega.4c11078
ACS Omega 2025, 10, 11296−11311

Histopathological Diagnosis of Liver Cancer Based on Raman Spectroscopy and Deep Learning. *Nat. Commun.* **2023**, *14* (1), 48.
(41) Su, N.; Dawuti, W.; Hu, Y.; Zhao, H. Noninvasive Cholangitis and Cholangiocarcinoma Screening Based on Serum Raman Spectroscopy and Support Vector Machine. *Photodiagn. Photodyn. Ther.* **2022**, *40*, 103156.

https://doi.org/10.1021/acsomega.4c11078
ACS Omega 2025, 10, 11296−11311